Open access • Journal Article • DOI:10.1116/1.1318668

Analysis of thin-film structures with nuclear backscattering and x-ray diffraction

— Source link

J. W. Mayer, King-Ning Tu

Institutions: Hodges University

Published on: 01 Jan 1974 - Journal of Vacuum Science and Technology (American Vacuum Society)

Topics: Silicide and Diffraction

Related papers:

- Growth Kinetics Observed in the Formation of Metal Silicides on Silicon
- Principles and applications of ion beam techniques for the analysis of solids and thin films
- Structure and growth kinetics of Ni2Si on silicon
- Formation kinetics and structure of Pd2Si films on Si
- Constitution of Binary Alloys

Share this paper:

View more about this paper here: https://typeset.io/papers/analysis-of-thin-film-structures-with-nuclear-backscattering-2r5jtw1s6w

Analysis of thin-film structures with nuclear backscattering and x-ray diffraction

J. W. Mayer*

California Institute of Technology, Pasadena, California 91109

K. N. Tu†

IBM Thomas J. Watson Research Center, Yorktown Heights, New York 10598
(Received 29 August 1973)

Backscattering of MeV ^{4}He ions and Seemann–Bohlin x-ray diffraction techniques have been used to study silicide formation on Si and SiO_2 covered with evaporated metal films. Backscattering techniques provide information on the composition of thin-film structures as a function of depth. The glancing-angle x-ray technique provides identification of phases and structural information. Examples are given of V on Si and on SiO_2 to illustrate the major features of these analysis techniques. We also give a general review of recent studies of silicide formation.

I. INTRODUCTION

The formation of silicide layers has played an important role in integrated circuit technology. Ohmic contacts and barriers on Si are formed by evaporating a metal layer (Pd, Pt, Ti, ...) on Si and by subsequent heating to form the metal-silicide.[1] We have utilized backscattering techniques with MeV He ions to study the kinetics of the silicide growth and glancing-angle x-ray diffraction techniques to identify the phases that are formed. This paper is a review of the capabilities of these analytical techniques and of the results obtained in our and other laboratories, concerning metal-silicon interactions.

The process steps of evaporation and heat treatment are simple and easily adapted to device production. The factors which govern the silicide formation are more complex. Of the 12 metal-silicon systems studied in some detail,[2–17] all have between three and seven silicide structures identified in bulk samples.[18–21] In thin-film structures, typically only one and in a few cases two silicide phases are formed. The lowest eutectic temperatures given in the phase diagrams range between 740 and 1400°C, yet the silicides form in thin-film samples at temperatures between 200 and 800°C. In most cases the formation occurs at temperatures of about one-third to one-half the melting point (in °K). This is a sure sign that solid-solid rather than solid-liquid reactions are involved. It has recently been found that silicide layers are formed during heat treatment of metal layers on SiO_2.[11,16] Usually, a different phase is formed and the reaction temperature is 100–200°C higher than for the metal-silicon systems.

From an operational standpoint it is of interest to determine the temperatures at which silicide growth occurs, the growth rates, the identity of the phases, their stability, and the influence of the interface conditions (presence of oxide layer). These aspects are of concern in integrated circuit technology and can be answered directly by the combined use of MeV He backscattering and glancing-angle x-ray diffraction techniques. The underlying problem is to determine what factors govern the nucleation and growth of the silicide. Some insight can be gained by measuring the kinetics of the process and determining which species, Si or metal, diffuses through the silicide layer. Again, backscattering techniques can be used.

II. ANALYTICAL TECHNIQUES

A. MeV ^{4}He Ion Backscattering

This technique has been described in detail previously[22–23] and will be discussed only briefly. As shown in Fig. 1, the sample is mounted in a chamber (modest vacuum requirements, $\sim 10^{-5}$–10^{-6} Torr) and bombarded with monoenergetic He ions (typically at 2 MeV) at current levels of 20–50 nA over about a 2×2-mm area. Only a small fraction of the incident particles are backscattered so the beam is to first order not attenuated. The silicon surface barrier detector produces a voltage pulse that is proportional to the energy of the individual backscattered He ions. The pulses are amplified and stored in a pulse-height

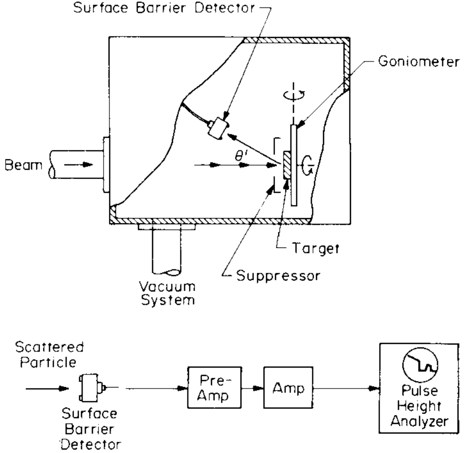

FIG. 1. Schematic diagram of the sample chamber used in backscattering measurements.

 Copyright © 1974 by the American Vacuum Society

analyzer, and at the end of the analysis (generally 15–30 min) the energy spectrum of backscattered particles is displayed.

The energy of particles scattered from surface atoms is determined by the mass of the target atom through scattering kinematics K (billiard-ball kinetics), the number of particles backscattered by the scattering cross section σ [Rutherford scattering with $\sigma \propto (Z/E)^2$ in this energy region], and the energy loss in traversing the film by stopping cross section ϵ. All these parameters, K, σ, and ϵ, are well known with the major uncertainty in the stopping cross section ϵ where the values are generally established within $\pm 5\%$.[24] Consequently, these backscattering spectra give directly and quantitatively the distribution of elements as a function of depth in the target. In effect it provides mass-sensitive depth microscopy.

It should be noted that the depth scale is determined by the number of target atoms/cm^2 in an incremental layer, not by the thickness of the layer. Cast in other terms, the density of a thin film can be determined from measurement of the number of target atoms/cm^2 (or from the difference in energy between particles scattered from the front and rear surface of a film) and from an independent measurement of the film thickness by interferometric techniques. For simplicity, the film thicknesses are usually given in dimensions of Å with the assumption of bulk density.

The advantages of backscattering then are (i) quantitative measurement of composition, (ii) nondestructive determination of depth profiles, and (iii) simple and direct interpretation of experimental data. The measurements themselves are quite easy to perform.

Some of these features are shown in Fig. 2, which gives backscattering spectra for an evaporated layer of V on Si before and after heat treatment. For the as-deposited case (dashed line), the broad peak is the component of the spectrum due to particles backscattered from V. The measured energy difference between particles scattered from the front surface and the back surface of the V layer—i.e., the width of the peak—is 300 keV, which corresponds to 2.24×10^{18} V atoms/cm^2 or a thickness of 3100 Å if bulk density is assumed. After heat treatment, a step appears in both the V and Si portions of the spectrum. This step

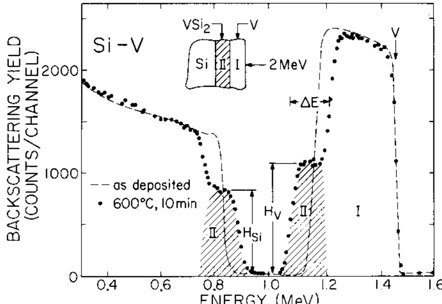

FIG. 2. Backscattering spectra for 2-MeV ^{4}He ions incident on Si sample covered with 3100 Å of V and heat treated at 600°C. Data from Kraütle *et al.* (Ref. 16).

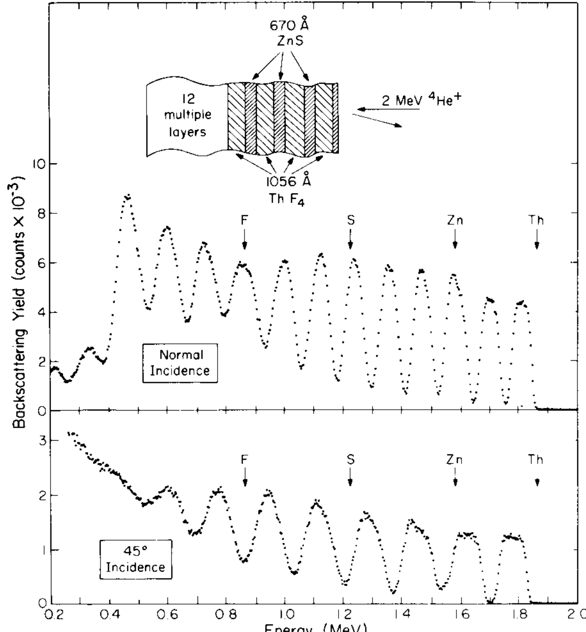

FIG. 3. Backscattering spectra for 2-MeV ^{4}He ions incident on a multilayer antireflecting coating on quartz substrate. There are 12 layers of ThF_4 separated by layers of ZnS (sample supplied by R. Honig, RCA).

corresponds to the formation of a silicide layer. The composition can be determined from the ratio of the heights, H, of the V and Si steps, here 1.35, when corrected for the ratio of scattering cross sections, $\sigma_{Si}/\sigma_V=0.36$. This gives a V/Si ratio of 0.485 which must be corrected upwards by a factor of 1.04 because of the differences in stopping cross section for particles scattered from V and from Si. This result shows that in the layer there are two Si atoms for every V atom, an indication that the compound VSi_2 is formed. However, positive identification requires structural data which are provided by x-ray diffraction (see Sec. II B).

The thickness t of the composite layer is determined from the energy width ΔE; here $\Delta E=140$ keV. In assuming bulk density this gives a thickness of 1700 Å. The growth kinetics of the composite layer can be found from the time dependence of ΔE for various heat treatment cycles.

The fact that the edges of the steps are sharp in Fig. 2 demonstrates that the layer is uniform in thickness over the dimensions of the beam. Laterally, nonuniformities introduce a broadening in the edges and hence uncertainties in thickness determination. If local cracking or flaking of the film occurs during thermal processing, backscattering spectra are misleading. Hence, one should also examine the lateral uniformity by optical microscopy or preferably by use of a scanning electron microscope.

Backscattering spectra are simple to interpret when there are only a few elements in the target. For multilayer targets, the spectra can be complex. Figure 3 shows spectra for normal incidence and 45° beam-to-target orientation for a 12-layer ThF_4-ZnS reflective coating. The distinct peaks reflect the Th in the 12

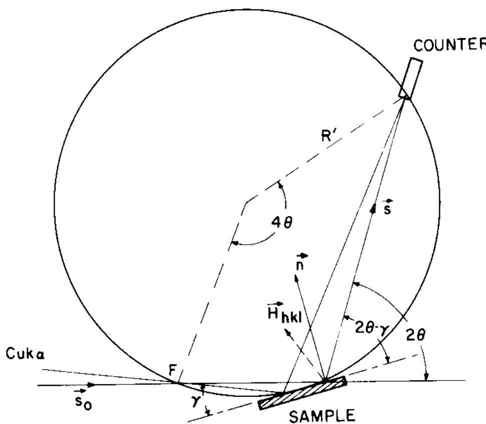

FIG. 4. Schematic diagram of the geometry of Seemann-Bohlin diffraction configuration.

ThF_4 layers, and the valleys show the position and thickness of the ZnS layers. The contribution from the Zn, S, and F cannot directly be seen in the spectra. The arrows indicate their energy position if located at the surface. The two peaks at the highest energy are flat topped and have sharp edges indicated well-defined layers of uniform composition. At lower energies (greater depths in the multilayer structure) the broadening of the edges reflect both a loss of depth resolution due to energy straggling and interference from lower-mass elements.

B. Seemann–Bohlin X-Ray Diffraction

The Seemann–Bohlin configuration for structural analysis of thin films is basically a glancing-angle x-ray diffraction using a focused beam with a fixed angle of incidence. It is known that to study the structure of a polycrystalline thin film of thickness of the order of 10^2–10^4 Å is difficult by conventional x-ray techniques because there is not much material for scattering. However, scattered beams can be strengthened by increasing the path of the x-ray in the film by the use of a fixed incident beam at a near-grazing incidence, and we note that such a fixed incident beam can be obtained in a diffractometer based on the focusing Seemann–Bohlin configuration but not on the conventional Bragg-Brentano configuration.[25] In the focusing Seemann–Bohlin configuration (see Fig. 4) the specimen is placed on the circumference of the diffraction circle and the angle of incidence is fixed and can be made as small as a few degrees; for example, an incident angle of 6.4° in this case will increase the length of the path of the beam in the specimen to about nine times its thickness. The specimen, the focus F of the monochromatic incident beam, and the focus of the diffracted beams all lie ideally on the circumference of the diffraction circle. Based on this principle, Feder and Berry[26] have designed and built an x-ray diffractometer with a diffraction circle of 20-in. diameter. An important feature of the diffractometer is that it employs a pyrolytic graphite monochromator crystal to produce a high-intensity monochromatic Cu K_α radiation as the incident beam. The intensity obtained from the graphite crystal is 15 times greater than that obtained from a LiF crystal. Also, a circular helium chamber of 18-in. diam is interposed in the path of the diffracted beams to reduce the atmospheric absorption.

The performance of the diffractometer has been discussed elsewhere.[26] We mention briefly here that it has detected a polycrystalline copper film of 150 Å and showed a precision lattice parameter measurement of a number of 1000-Å nickel films with an accuracy of ± 0.0001 Å—i.e., 1 part in 35 000. In addition to the high sensitivity of detecting phases, the Seemann–Bohlin diffraction allows convenient structural analysis of grain size, biaxial strain, and the distribution of pole densities. This is because its reciprocal lattice vector H of Bragg diffractions is not parallel to the normal n of the film surface but rather makes inclination angles with the normal. The angle increases with the order of the reflections. Thus each reflection measures in a different direction the lattice parameters, the size, and the total amount of coherently diffracted regions. It is clear that this type of diffractometer can deliver a great deal of structural information of polycrystalline thin films. We should note that single-crystal films are not suitable for a Seemann–Bohlin diffractometer and the diffraction patterns may show no peaks at all. This may be regarded as advantageous for a polycrystalline film on a single-crystal substrate such as a metal film on a Si wafer since we do not need to worry about the interference of Si reflections.

It seems that for a structural study of thin films of thickness around 1000 Å and less we can use transmission electron microscope, for films thicker than several microns we can use conventional x-ray equipment, and for films in between we can use a Seemann–Bohlin-type x-ray diffractometer.

The diffractometer is expected to be very powerful in the investigation of the interaction in thin films[27] because the reaction products can be identified by their x-ray reflections very early in the diffusion cycle. Figure 5 shows the x-ray pattern of a sample of 3200 Å of V on a Si wafer that has been heat treated at 800°C for 15 min. The pattern was obtained by scanning the sample with Cu K_α radiation at steps of 0.15° (4θ)

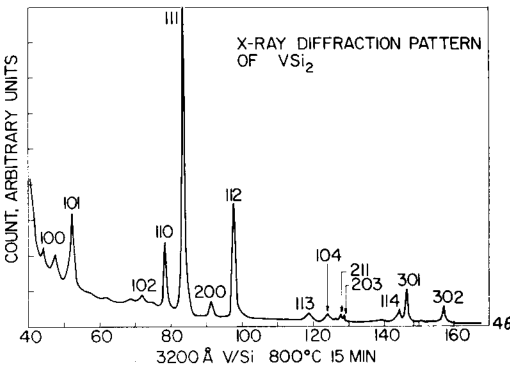

FIG. 5. X-ray diffraction pattern of V-Si heat treated at 800°C for 13 min in an oxygen-free furnace. The vanadium film had a thickness of 3200 Å. Reflections of VSi_2 are indexed.

increment and with a counting time of 30 sec at each step. The peaks have been indexed as reflections of VSi_2 according to ASTM Card No. 13-260. In this sample, the x-ray diffraction data confirm the composition analysis determined from backscattering data (Fig. 2).

III. ANALYSIS OF SILICIDE FORMATION

A. General Precautions

One of the objectives of this type of analysis is to determine the growth kinetics. It is a course fraught with peril, and sample preparation is the dominant factor. There are three areas which must be considered: interface, contamination, and stress.

1. *Interface.* The native oxide layer on silicon surfaces must be considered when preparing samples. It has been shown that thin oxide layers significantly retard silicide formation.[6] The thickness of a native oxide layer is markedly different for different wafer orientations,[28] and hence sample orientation plays a role. Soaking in HF and then rinsing prior to mounting in the evaporation chamber does not guarantee an oxide-free surface. One approach is to sputter clean the surface and then to deposit the metal layer without breaking vacuum. Although this creates reproducible surface conditions, the silicon surface is heavily damaged and the sputtering gas is retained in the surface layer.[29]

2. *Contamination.* Oxygen and other ambient contaminations can be introduced during deposition or thermal processing. Trace inclusions of oxygen are hard to detect by backscattering techniques, although relatively massive concentrations (10–20 at.%) can be readily identified. There has not been a positive correlation of film contamination with retardation of silicide growth; however, preliminary data suggest that this may be a real problem.[30]

3. *Stress.* One of the most difficult factors to overcome is film cracking or peeling due to stress created during thermal processing. Backscattering measurements on such samples are unreliable. Film peeling is often enhanced for thicknesses greater than a few thousand angstroms. In some cases, this problem can be alleviated by maintaining an oxide-free interface or depositing the film at elevated temperatures.

There is of course the polycrystalline nature of the deposited and reacted film that should be considered. Grain size and grain boundary diffusion may be important particularly at low process temperatures ($T \lesssim 400°C$). These problems have not been properly addressed in silicide formation, but are known to occur in metal-metal thin-film studies. At higher temperatures, bulk diffusion will probably dominate over grain boundary effects.

B. An Example: V-Si System

Backscattering analysis has been applied to nearly a dozen silicide systems, two of which (Pd–Si[3,6,9,10,12–14] and Hf–Si[7,8]) have been studied in detail. We have chosen the vanadium-silicide system as an example because the problems are still fresh (as the study has not been completed), and also we can consider aspects of silicide formation on SiO_2. Our work[11,16] with Ti, Nb, and V deposited on SiO_2 shows that silicides are formed but at higher process temperatures than for Si/metal systems and that the silicide is metal rich.

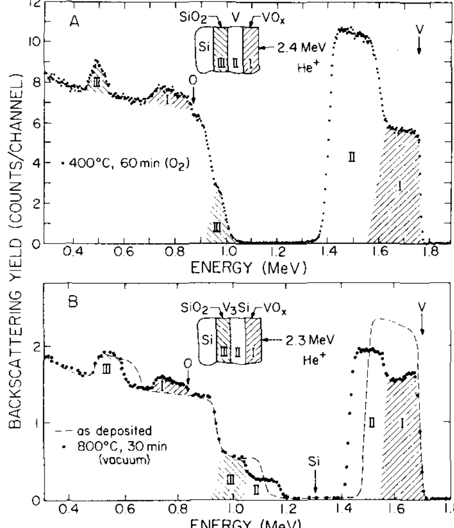

Fig. 6. Backscattering spectra for 2.3-MeV ^4He ions incident on a Si sample with a thermally grown layer of SiO_2 covered with an evaporated layer of V. (a) heat treatment at 400°C for 60 min in O_2 ambient, and (b) heat treatment at 800°C for 30 min in vacuum. Data from Kraütle *et al.* (Ref. 16).

Figure 6 shows backscattering spectra for V films deposited on SiO_2.[30] For the as-deposited case [dashed line in Fig. 6(b)], the spectrum shows the contribution from V and Si in the oxide layer and substrate, and from oxygen in the oxide layer. The oxygen contribution is superimposed on that from the underlying Si substrate. The arrows indicate the energy position of these elements when at the surface. After heat treatment in oxygen at 400°C, there is a change in the composition of the sample. Oxygen is now present at the outermost layers (I) as is evident in Fig. 6(a) from the step in the V component and the appearance of a broad mesa whose high-energy edge corresponds to the position of oxygen at the surface. There is not a significant amount of oxygen in underlying V layer (II) as is indicated by the following: (a) The height of the V portion of the spectrum (layer II) coincides with the as-deposited case; and (b) there is a dip in the oxygen component of the spectrum in the region between that from oxygen in SiO_2 (III) and in vanadium oxide (I).

The composition of the vanadium oxide can be estimated from the ratio of the heights of vanadium and oxygen components in region I to be close to that of V_2O_5. Positive identification was made from glancing-angle x-ray diffraction data (Fig. 7). The peaks correspond to those indexed for V_2O_5.

With reference again to Fig. 6, it is evident that there is a dramatic change in composition when a similar sample is heated to 800°C in vacuum. The composition of the layers can be deduced from the spectrum to

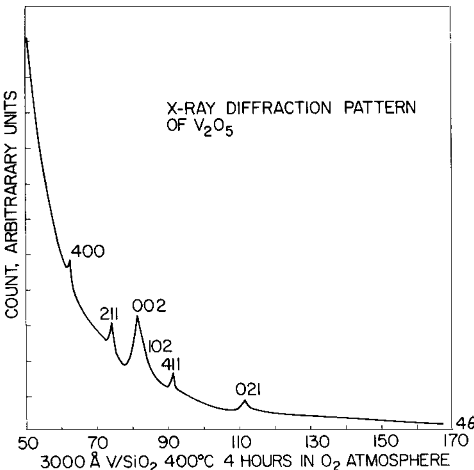

FIG. 7. X-ray diffraction pattern of V-SiO_2 heat treated at 400°C for 4 h in an atmosphere of O_2+H_2O. The vanadium film had a thickness of 3000 Å. Reflections of V_2O_5 are indexed.

show the following: for *layer I*, approximately equal amounts of vanadium and oxygen with no appreciable concentration of Si; for *layer II*, three times as much V as Si and no appreciable oxygen; for *layer III*, SiO_2 but of reduced thickness. The amount of oxygen removed from the initial thickness of SiO_2 (III) corresponds to the amount added to the vanadium oxide layer (I), which indicates that the amount of oxygen in the composite layers is conserved.

The x-ray diffraction data for this sample coincide with those given by Tu *et al.*[11] for a similar sample and show the presence of V_3Si, V_5Si_3, and V_2O_5. The major feature is the predominance of V_3Si for this sample, whereas VSi_2 is formed in the V-Si samples.

There are two unusual features in this comparison between backscattering and x-ray diffraction data. Backscattering data indicate a 1:1 ratio of V to O, and diffraction data indicate V_2O_5. This may be due to the fact that the V_2O_5 eutectic is at a lower temperature[18] then the 800°C process temperature. We suggest that oxygen dissolves in the vanadium at the process temperature and then the V_2O_5 nucleates as crystallites imbedded in a matrix of vanadium when the sample cools below the eutectic. However, the average V/O ratio over the entire vanadium-oxide film thickness could be near unity as indicated by backscattering data.

TABLE I. Comparison of silicide formation in thin metal films deposited on Si. The numbers in parenthesis indicate the temperature at which silicide formation was observed by backscattering techniques. The asterisks indicate silicides that have been identified by diffraction techniques.

IV B	V B	VI B	VIII
Ti*	V	Cr	Ni NiSi (600°C)
$TiSi_2$ (600°C)	VSi_2 (600°C)	$CrSi_2$ (450°C)	$NiSi_2$ (800°C)
Zr	Nb	Mo	Pd* Pd_2Si (200°C)
$ZrSi_2$ (700°C)	$NbSi_2$ (650°C)	$MoSi_2$ (1200°C?)	PdSi (740°C)
Hf* HfSi (550°C) $HfSi_2$ (750°C)	Ta	W WSi_2 (650°C)	Pt* Pt_2Si (200°C) PtSi (300°C)

The other question concerns the location of the V_5Si_3 identified in x-ray diffraction. Backscattering data[16] do not show appreciable amounts of Si near the surface [region I in Fig. 6(b)] and the spectrum height ratio for the silicide layer (region II) corresponds to V_3Si. At present we suggest the V_5Si_3 is located near the interface between regions I and II.

This example clearly shows the drastic effect that a thin oxide can have on both growth kinetics and silicide composition. In this case, the metal-rich silicide is of interest in its own right as a superconductor with a transition temperature of 17°K.[11]

IV. SILICIDE FORMATION

In this section we will review experimental data on silicide formation from the standpoint of structure, thermodynamics, and kinetics. We also include some speculations and suggestions for future work. Table I gives a general impression of results obtained, and more details are given in Table II.

A. Structure

The typical silicide which is formed with metal-Si interaction is the phase which is most rich in Si—i.e., PtSi and $CrSi_2$. This is the end point which one expects from an equilibrium point of view. There should be two phases, Si and the most Si rich silicide. It is surprising that more phases do not appear, as one would expect all phases to be present during the reaction stage. Indeed, intermediate phases (Pd_2Si, Pt_2Si, HfSi, and NiSi) have been detected in a few systems. Other phases may be present, but their extent is determined from kinetic considerations of diffusion rate and nucleation. Kidson[32] had earlier pointed out that if the rate constants of diffusion in a given phase are small the phase layer may be too thin to be detected.

The microstructure of HfSi, $HfSi_2$, VSi_2, PtSi, and Pd_2Si has been measured by x-ray diffraction. As a first approximation, the grain size of the silicide is about the same as that of the deposited metallic film (~200–500 Å). There have not been serious attempts to measure strain in the silicide layer and its dependence on heat treatment temperature. This is clearly one area that should be explored further.

Even though the crystal structure of most silicides are different from Si, they tend to show some preferred orientation. The most striking case is Pd_2Si, which has been shown by both reflection-electron diffraction and MeV $^4He^+$ channeling techniques to grow epitaxially on ⟨111⟩ Si.[10,12–14] In this case, the hexagonal basal plane of Pd_2Si matches quite well with the ⟨111⟩ Si structure. Similar considerations of lattice matching suggest that $NiSi_2$, $CoSi_2$, and $FeSi_2$ may also form epitaxially. This conclusion has not been tested and is an obvious area for further study.

B. Thermodynamics

Silicide formation energies have been tabulated[33] for the following four systems: Mo-Si, Ta-Si, Ti-Si, and

TABLE II. Silicide formation.

Metal[a]	Phases	Structure	Backscattering Phase	Backscattering T_{obs} (°C)	Backscattering Kinetics	T_{melt} (°C)	T_{obs} (K) / T_{melt} (K)	Reference
Ti (3)	Ti_5Si_3	hexagonal				2120		
	TiSi	orthorhombic				1700		
	$TiSi_2$	orthorhombic (C49)	$TiSi_2$	600	$t^{1/2}$	1540	~0.5	6
Zr (7)	Zr_2Si	tetragonal				2110		
	ZrSi	orthorhombic				2095		
	$ZrSi_2$	orthorhombic (C49)	$ZrSi_2$	700		1520	~0.5	15
Hf (5)	Hf_2Si	tetragonal				2430		
	HfSi	orthorhombic or hexagonal (FeB)	HfSi	550	$t^{1/2}$	2200	~0.3	
	$HfSi_2$	orthorhombic (C49)	$HfSi_2$	750		1900	~0.5	7, 8
V (3)	V_3Si	cubic (β-W)				2070		
	V_5Si_3	tetragonal (D8m)				2150		
	VSi_2	hexagonal (C40)	VSi_2	600	$t^{1/2}$	1750	~0.5	11, 16
Nb (4)	Nb_4Si	hexagonal						
	Nb_3Si	cubic (Cu_3Au)						
	$NbSi_2$	hexagonal (C40)	$NbSi_2$	650			~0.5	31
Ta (3)	Ta_2Si	tetragonal (Al_2Cu)				2460		
	$TaSi_2$	hexagonal (C40)				2200		
Cr (5)	Cr_3Si	cubic (β-W)				1730		
	CrSi	cubic (FeSi)				1600		
	$CrSi_2$	hexagonal (C40)	$CrSi_2$	450	t	1550	~0.4	6, 15
Mo (3)	Mo_3Si	cubic (β-W)				2120		
	$MoSi_2$	tetragonal (C11b)	$MoSi_2$	1200	t	2050	~0.6	6
W (2)	W_3Si_2	tetragonal				2350		
	WSi_2	tetragonal (C11)	WSi_2	650	$t^{1/2}$	2165	~0.35	17
Ni (6)	Ni_3Si	cubic (Cu_3Au)				1165		
	NiSi	orthorhombic (MnP)	NiSi	600		992	~0.7	
	$NiSi_2$	cubic (CaF_2)	$NiSi_2$	800		993	~0.85	15
PD (3)	Pd_3Si	orthorhombic (Fe_3C)				960		
	Pd_2Si	hexagonal (Fe_2P)	Pd_2Si	200	$t^{1/2}$	1330	~0.35	3, 6, 9, 10, 12–14
	PdSi	orthorhombic (MnP)	PdSi	735		1090	~0.75	14
Pt (5)	Pt_3Si	monogonal				870		
	Pt_2Si	hexagonal (Fe_2P)						
		tetragonal (Al_2Cu)	Pt_2Si	200	$t^{1/2}$	1100	~0.4	
	PtSi	orthorhombic (MnP)	PtSi	200	$t^{1/2}$	1229	~0.35	4, 5

[a] The number in parentheses indicates the number of phases found in bulk samples (Refs. 18–20).

Zr-Si. In the Mo-Si system, $MoSi_2$ is the most stable phase among the Mo-silicides and was found to be the predominant phase in backscattering measurements. $TaSi_2$ is equally stable as compared to the Ta-silicides; however, there have been no measurements of silicide formation in evaporated Ta films on Si. For the Ti-Si and Zr-Si systems, the monosilicides TiSi and ZrSi have lower free energies than the disilicides $TiSi_2$ and $ZrSi_2$. This suggests that before the formation of the disilicide an intermediate stage might be observed. There is no direct evidence for this, although our preliminary results[34] on Ti-Si hint at the presence of an intermediate phase before $TiSi_2$ is formed. In the Hf-Si system, which should be analogous to Zr-Si, HfSi does form and is stable up to temperatures of ~750°C, where $HfSi_2$ forms. In spite of these indications, we believe that there is not yet sufficient evidence to make a strong correlation with formation energy. This situation might be improved if measurements were made on the Ta-Si system and if further measurements were carried out in the Mo-Si system.

From a conventional standpoint, the stability of a phase is indicated by its melting point. This may be misleading and should not be used as a guide to predict which forms first. It is interesting to note, however, from Table II that a value of half the melting point in °K is a rough guide to the minimum temperature at which silicide formation has been observed. This may be too high an estimate because HfSi, Pd_2Si, WSi_2, and PtSi form at about one-third the melting point. In fact the one-third relation may be the rule rather than the exception because oxide layers at the interface will raise the formation temperature. For example, the published NiSi formation temperature of 600°C is higher than that of 300°C recently obtained in a separate investigation.[34] We suspect that the presence of the native oxide layer on Si might be responsible for the high temperature found for the Mo-Si system.

We can consider other aspects such as epitaxial growth that might effect stability. Hutchins and Shepala[12] showed for transformation of Pd_2Si to PdSi that higher temperatures are required on ⟨111⟩-oriented

Si than on ⟨100⟩. On ⟨111⟩-oriented Si, Pd_2Si shows the strongest orientation. While Pd_2Si is very stable (200–700°C), Pt_2Si is not and transforms to PtSi quite easily. One reason might be that Pd_2Si is epitaxial and has a higher melting point than PdSi, while Pt_2Si does not show good epitaxy and has a lower melting point than PtSi.

For Pt_2Si one finds the low-temperature (tetragonal) phase in these silicides rather than the high-temperature (hexagonal) phase; the polymorphic transition temperature is at about 700°C. We attempted to form this hexagonal phase (which should be epitaxial on ⟨111⟩ Si) by heating a sample to 750°C for 30 min. Backscattering data[34] showed that PtSi (3% Si rich) rather than Pt_2Si was formed. Consequently, this attempt to form a more stable phase of Pt_2Si was not successful.

C. Kinetics

From the standpoint of kinetics, the important factors are the mechanisms for transporting metal or Si across the silicide layer, the activation energy, and the identity of the diffusing species. Most silicides tend to react at temperatures above 500–600°C, except for the Pd-Si and Pt-Si systems, which react at temperatures as low as 200°C. The activation energy measured for the growth process for these latter silicides is between 1.1 and 1.5 eV. This is remarkably low and opens the question of grain boundary growth. We believe, however, that bulk diffusion dominates. The structure of Pd_2Si is very open, and interdiffusion is expected to be fast. Furthermore, the same activation energy was found from 100 to 700°C, indicating that the same diffusion mechanism was involved. Also, the same growth rate is found for Pd_2Si on differently oriented Si samples where the amount of epitaxy is different. In cases where there is less epitaxy, one anticipates more large-angle grain boundaries and increased grain boundary diffusion. All these findings support the dominance of bulk diffusion even at temperatures of 200°C.

The other silicides react at higher temperatures, and we would expect lattice diffusion to be dominant. The activation energy for diffusion has only been measured in a few cases, but it seems to be above 2 eV (2.5 eV for HfSi, 2.9 for VSi_2, and 2.7 for WSi_2). These values are too high for grain boundary diffusion and suggest bulk effects. One would expect to see grain boundary diffusion at lower temperatures. This could be tested by prolonged heating of a sample at temperatures below the reaction temperatures and by looking for Si accumulation at the free surface. This interface accumulation is often seen in backscattering studies of metal-metal interactions at low temperatures. However, no systematic studies have been made on metal-Si systems.

The growth of most silicides (HfSi, Pd_2Si, Pt_2Si, PtSi, $TiSi_2$, WSi_2, and VSi_2) has been found to follow a $(\text{time})^{\frac{1}{2}}$ relationship characteristic of a diffusion-dominated process. In two cases, $CrSi_2$ and $MoSi_2$, a linear growth has been found.[6] These systems have not been studied in detail, and we cannot speculate on the reasons for the linear growth rate. In fact, the growth kinetics of all the high-temperature silicides has not been followed in as much detail as has been done for Pd-Si and Pt-Si. There is a need for careful kinetic studies on samples with oxide-free interfaces between metal and Si.

There is one other notable gap in all the data. With the exception of HfSi, there is no evidence to indicate whether Si or metal is the diffusing species through the silicide layer. This datum could be obtained by implanting rare gas atoms into the silicide and by using backscattering techniques to determine whether the gas atoms move toward or away from the surface. Similar studies have been made with anodic oxidation.[35] For the Hf–Si system, the argon that was present as an impurity introduced during deposition served as a marker.[7] The data indicated the Si was the diffusing species. There are practical implications. If Si is the diffusing species, it will leave vacancies near the Si–silicide interface. If these vacancies condense into voids, it leads to easy peeling of the silicide under stress.

D. Comparison with M/SiO_2 Reactions

It has recently been found that the silicide formation can occur with metals in contact with SiO_2.[11,16] The behavior of V–SiO_2 and V–Si has been discussed in Sec. III B. In the case of Ti, Nb, and V the silicide was the more metal-rich phase.[16] At present our work is in too early a stage to give any insight into this behavior. One immediate question is to determine if the Si-rich phase forms when the SiO_2 layer is consumed.

V. SUMMARY

This review was intended as a survey of metal-silicide formation studies where both backscattering and x-ray diffraction measurements have been utilized. These techniques complement each other as backscattering data give composition as a function of depth and, hence, can be used to determine growth kinetics while x-ray diffraction gives identification of phases and structural information.

A survey of silicide formation for metal films deposited on Si indicates that the typical silicide that is formed is the phase that is most rich in Si. This is the end point one expects from thermodynamic equilibrium considerations. In some cases intermediate phases have been found. On the basis of present data we have not been able to find general guidelines that can be used to predict when such an intermediate phase will occur. One striking observation is that metal-rich silicides are formed when the metal layer is deposited on SiO_2 rather than on Si.

The formation temperature on the silicides is generally between one-third to one-half the silicide melting point in °K. This shows that solid-solid rather than solid-liquid reactions are involved. The growth kinetics

of the silicide with two exceptions have been found to follow a (time)$^{1/2}$ dependence typical of diffusion-limited reactions. We believe that bulk rather than grain boundary diffusion is involved. There have not been studies to determine whether the metal or the Si is the diffusing species, except for the Hf-Si case where Si appeared to migrate.

Our survey indicates that only the most general features of silicide formation have been studied. There are a number of areas that require further investigation. Until these are carried out, it is difficult to present an over-all picture of the factors which control silicide formation.

ACKNOWLEDGMENT

The authors acknowledge with pleasure discussions with our colleagues: C. J. Kircher and J. F. Ziegler at IBM; M-A. Nicolet, W-K. Chu, and H. Kraütle at Caltech. The authors also thank H. Kraütle for his data on V-Si and V-SiO_2.

*Work supported in part by A. F. Cambridge Research Laboratories.

†Work supported in part by ARPA Contract No. F19628-73-C-0006 administered by AFCRL.

[1]M. P. Lepselter and J. M. Andrews, in *Ohmic Contacts to Semiconductors*, edited by B. Schwartz (The Electrochemical Society, New York, 1969), p. 159.
[2]M. P. Lepselter and S. M. Sze, Bell Syst. Tech. J. **47**, 89 (1969).
[3]C. J. Kircher, Solid-State Electron. **14**, 507 (1971).
[4]A. Hiraki, M-A. Nicolet, and J. W. Mayer, Appl. Phys. Lett. **18**, 178 (1971).
[5]H. Muta and D. Shinoda, J. Appl. Phys. **43**, 2913 (1972).
[6]R. W. Bower and J. W. Mayer, Appl. Phys. Lett. **20**, 359 (1972).
[7]C. J. Kircher, J. W. Mayer, K. N. Tu, and J. F. Ziegler, Appl. Phys. Lett. **22**, 81 (1973).
[8]J. F. Ziegler, J. W. Mayer, C. J. Kircher, and K. N. Tu, J. Appl. Phys. **44**, 3851 (1973).
[9]R. W. Bower, R. E. Scott, and D. Sigurd, Solid-State Electron. (to be published).
[10]D. Sigurd, W. Van der Weg, R. Bower, and J. W. Mayer, Thin Solid Films (to be published).
[11]K. N. Tu, J. F. Ziegler, and C. J. Kircher, Appl. Phys. Lett. **23**, 493, (1973).
[12]G. A. Hutchins and A. Shepala, Thin Solid Films (to be published).
[13]D. H. Lee, R. R. Hart, D. A. Kiemet, and O. J. Marsh, Phys. Status Solidi A **15**, 645 (1973).
[14]W. D. Buckley and S. C. Moss, Solid-State Electron. **15**, 1331 (1972).
[15]K. E. Sundström, S. Petersson, and P. A. Tove, Uppsala University Report No. UPTEC 73-29R (unpublished).
[16]H. Kraütle, M-A. Nicolet, and J. W. Mayer, Phys. Status Solidi A (to be published).
[17]J. A. Borders and J. N. Sweet, private communication.
[18]M. Hansen, *Constitution of Binary Alloys* (McGraw-Hill, New York, 1958).
[19]R. P. Elliott, *Constitution of Binary Alloys, First Supplement* (McGraw-Hill, New York, 1965).
[20]F. A. Shunk, *Constitution of Binary Alloys, Second Supplement* (McGraw-Hill, New York, 1969).
[21]W. B. Pearson, *Handbook of Metals and Alloys* (Pergamon, Oxford, 1967), Vol. 2.
[22]M-A. Nicolet, J. W. Mayer, and I. V. Mitchell, Science **177**, 841 (1972).
[23]W. K. Chu, J. W. Mayer, M-A. Nicolet, T. M. Buck, G. Amsel, and F. H. Eisen, Thin Solid Films **17**, 1 (1973).
[24]W. K. Chu, J. F. Ziegler, I. V. Mitchell, and W. D. Mackintosh, Appl. Phys. Lett. (to be published).
[25]B. D. Cullity, *Elements of x-ray Diffraction* (Addison-Wesley, Reading, Mass., 1956).
[26]R. Feder and B. S. Berry, J. Appl. Cryst. **3**, 372 (1970).
[27]K. N. Tu and B. S. Berry, J. Appl. Phys. **43**, 3283 (1972).
[28]W. K. Chu, E. Lugujjo, J. W. Mayer, and T. Sigmon, Thin Solid Films (to be published).
[29]G. W. Sachse, W. E. Miller, and C. Gross (unpublished).
[30]H. Kraütle, private communication.
[31]C. J. Kircher and J. F. Ziegler, private communication.
[32]G. V. Kidson, J. Nucl. Mater. **3**, 21 (1961).
[33]R. Hultgren, R. L. Orr, and K. Kelley, *Supplement to Selected Values of Thermodynamic Properties of Metals and Alloys* (Department of Mineral Technology, University of California, Berkeley, Calif., 1968.
[34]K. N. Tu and W. K. Chu (unpublished).
[35]F. Brown and W. D. MacKintosh, J. Electrochem. Soc. (to be published).